



HAL
open science

Numerical Assessment of Thermal Performance and Heat Storage Capacity of Thermoactive Geostructures

Yvon Delerablee, Sebastien Burlon, Philippe Reiffsteck, Eric Antoinet

► **To cite this version:**

Yvon Delerablee, Sebastien Burlon, Philippe Reiffsteck, Eric Antoinet. Numerical Assessment of Thermal Performance and Heat Storage Capacity of Thermoactive Geostructures. SEG 2018, International Symposium on Energy Geotechnics, Sep 2018, Lausanne, Switzerland. pp 11-18, 10.1007/978-3-319-99670-7_2 . hal-03572555

HAL Id: hal-03572555

<https://hal.science/hal-03572555>

Submitted on 14 Feb 2022

HAL is a multi-disciplinary open access archive for the deposit and dissemination of scientific research documents, whether they are published or not. The documents may come from teaching and research institutions in France or abroad, or from public or private research centers.

L'archive ouverte pluridisciplinaire **HAL**, est destinée au dépôt et à la diffusion de documents scientifiques de niveau recherche, publiés ou non, émanant des établissements d'enseignement et de recherche français ou étrangers, des laboratoires publics ou privés.

Numerical assessment of thermal performance and heat storage capacity of thermoactive geostructures

Yvon Delerablee^{1*}, Sebastien Burlon², Philippe Reiffsteck², Eric Antoinet¹

¹ Antea Group, Antony, 92160, France

² University of Paris-Est, The French Institute of Science and Technology for Transport, Development, and Networks (IFSTTAR), Marne La Vallée, 77447, France

*corresponding author: yvon.delerablee@anteagroup.com

Thermoactive geostructures represent an original technique to fulfil energy demand of buildings and infrastructure. The thermal performance of such structure depends on several parameters as the thermal solicitation, the hydrogeological context and the thermal characteristics. To improve the design of the thermoactives geostructures, an original approach based on the analysis of thermal flux and volumetric thermal power has been developed. This method permits to assess the temperature variation of a volume and the potential thermal drift of the system. Moreover, this method is used to analyse the thermal behaviour of thermoactive diaphragm walls.

1. Introduction

Thermoactives geostructures aim at the production of heating during winter and cooling during summer and include various geotechnical structures with embedded heat exchanger tubes. This technology can also be implemented in deep foundations, retaining walls, base slab and tunnels (CFMS and SYNTEC, 2017). Since its development during the years 1980 (Brandl, 2006), the complexity of the structures equipped with heat exchanger tubes increases continuously and now one of the current challenge concerns the installation of these tubes in more complex structures as metro stations and tunnels (Barla et al, 2016).

The design of geotechnical structures requires to consider thermal stress and strain and the interactions between mechanical and thermal effects. Many studies have been carried out to study the thermo-mechanical behaviour of ground (Campanella and Mitchell, 1968; Laloui and Cekerevac, 2008) and thermal piles (Bourne-Webb et al, 2009; Adam and Markiewicz, 2009; Di Donna et al, 2016). From the thermal point of view, two study scale can be defined: the heat exchanger scale and the structure scale in its environment. The first issue has mobilized many research efforts from decades for the development of vertical borehole heat exchanger (Pahud et al, 1999). The second issue is related to the long-term behaviour of ther-

moactive geostructure and ground in terms of temperature variations and heat exchanges. The influence of the groundwater flow is of major importance to assess the potential thermal plume and the natural thermal recharge. At this scale, the heat exchanges are governed by (i) the thermal conductivity through the concrete and the ground, (ii) the groundwater flow velocity that affects the thermal recharge and the heat exchange by advection (Fromentin *et al.*, 1997; Barla *et al.*, 2016), (iii) the temperature variation of the external air and (iv) the 3D shape of the structure that has an influence on the groundwater flow.

Some approaches considering the building scale have been developed to simulate thermal response tests (Signorelli *et al.*, 2007; Zarrella *et al.*, 2017) and can be applied to thermoactive geostructures (Xia *et al.*, 2012). Based on these studies, three main issues in terms of design can be dealt with: what are the long-term effects on the ground and on the groundwater? What is the real heat exchange between the ground and the structure? What are the contributions of conduction and advection in term of heat exchange related to the groundwater flow velocity?

In this paper, an original approach based on the study of the heat fluxes induced by conduction and advection and their contributions to volumetric thermal power is developed to assess the long-term behaviour of such structure and especially thermoactive diaphragm walls. It is illustrated with an example of Paris metro station.

2. Assessment of thermal exchanges by conduction and advection

2.1 Analysis of the energy balance equation

The energy balance equation governing the heat exchange between the ground and the structure includes the contributions of conduction and advection:

$$C_{eff} \frac{\partial T}{\partial t} + \text{div}(\vec{j}_{cond}) + \text{div}(\vec{j}_{adv}) - j_{int} = 0 \quad (1)$$

where C_{eff} is the effective specific heat ($J/m^3.K$), T the temperature (K), j_{cond} the conductive heat flux (W/m^2), j_{adv} the advective heat flux and j_{int} the production of intern volumetric heat (W/m^3) which is usually neglected regarding the low depth of the structures.

The theorem of Green-Ostrogradski links the flux to the divergence of the heat fluxes:

$$\oint_{\partial V} \vec{j} \cdot d\vec{S} = \iiint_V \vec{\nabla} \cdot \vec{j} dV \quad (2)$$

The direct calculation of the different component of the heat fluxes in 3D is complex. From the divergence calculation, the inlet and the outlet fluxes are calculated to characterise the heat exchange across a volume. It is also a way to analyse the temperature variations. Indeed, when the sign of the divergence is negative, resp. positive, the temperature increase, resp. decrease. The higher the divergence is, the faster the increase/decrease is. Moreover, at steady state, the sum of the divergence is null which implies that the inlet heat flux is equal to the outlet heat flux. It means that, at null divergence, the energy of the system does not vary anymore and cannot gain or lose energy.

2.2 Application to the thermoactives geostructures

The divergence approach provides the thermal fluxes through a control volume defined by the first meter of ground close to the walls of the metro station (see Fig. 1). The control volume is defined to consider the heat exchange in every direction. The integration of the divergence on the control volume correspond to the thermal exchange at the time t between the ground and the structure $P_{tot}(t)$:

$$div(\vec{j}_{tot,i}(t)) = div(\vec{j}_{cond,i}(t)) + div(\vec{j}_{adv,i}(t)) \text{ at any point} \quad (3)$$

$$P_{tot}(t) = \sum_{i=1}^n V_i div(\vec{j}_{tot,i}(t)) \text{ for the control volume} \quad (4)$$

where n is the number of subdivisions of the volume and V_i the volume of the subdivision i (m^3).

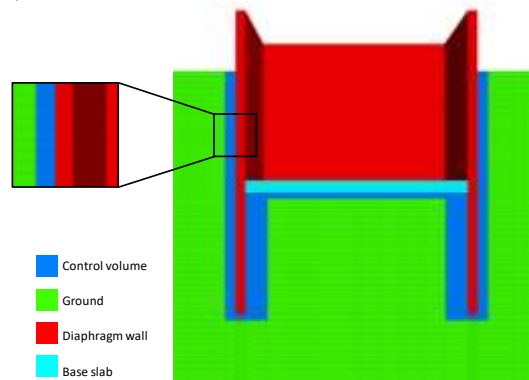


Fig. 1: example of control volume around diaphragm wall

It is also possible to define a volume to assess the energy balance and predict a thermal drift.

3. Numerical analysis

3.1 Methodology

3.1.1 Introduction

Within the framework of the diaphragm wall, it is essential to consider 3D effects. Indeed, the geometry of the underground structure can modify the initial characteristics of the groundwater flow (intensity and direction). It is called the dam effect. As the heat flux by advection is proportional to the groundwater flow velocity, the heat fluxes at the interface ground/structure are function of the dam effect. Therefore, the heat exchange can vary for each diaphragm wall.

In the model, some local variables can be calculated: heat fluxes $\vec{j}(x, t)$ (W/m^2), divergence of the heat fluxes $\text{div}(\vec{j}(x, t))$ (W/m^3), temperature $T(x, t)$ (K), groundwater flow velocity $\vec{v}_D(x, t)$ (m/s), heat exchange $P(x, t)$ (W), etc. Moreover, some global variables at the structure scale can be computed: global heat exchange $P_{tot}(t)$ (W), global mean heat flux $\Phi(t)$ (W/m^2) or by wall (see Fig. 3), thermal drift, etc. To represent the results of the simulations, it is also possible to define temporal means, as the daily annual mean of global heat exchange $\bar{P}_{tot,year}$ ($\text{W}_{\text{day/year}}$) and the seasonal annual mean of heat fluxes $\bar{\Phi}_{year}$ ($\text{W}/\text{m}^2_{\text{3month/year}}$).

It is essential to note that the main input data of the thermal solicitation of the thermoactive geostructure is the heating and cooling demand of the building. Indeed, the main goal is to determine how the ground reacts when this demand is satisfied partially or not. It is why the peak of demand and the global quantity of energy shall be considered. Indeed, a high peak demand is possible on a short period if the heat reservoir allows it. Within the framework of the thermoactives geostructures, the heat reservoir is the ground and the heat exchanges between the geostructure, the heat pump and the ground are only efficient if the ground can provide the right amount of heat. If it is not the case, the heat pump compensates with electric energy, decreasing its coefficient of performance.

3.1.2 Initial conditions

The calculations are performed with the software FLAC3D (ITASCA, 2013). The main assumptions considered are the following: the variation of the external air temperature, a desaturated zone in the subsurface and a convective heat flux between the internal air of the structure and the walls. In a first step, the groundwater flow is initialised to simulate the dam effect. In a second step, the temperature in the ground is initialised according to the groundwater flow, the external air temperature variations and the heat exchanges between the internal air

and the wall, before thermal activation of the structure. In this case, the external air temperature variations are governed by a sinusoidal signal.

Thereby, the temperature is equal to 14°C from about ten-meter depth. However, in the first meters, the ground temperature is function of the depth. Regarding the classical geometry of diaphragm walls (< 60 m depth), a non-negligible part of the structure is influenced by the external air temperature variations.

The thermal solicitation is applied as a nodal power in the plan of the heat exchanger tubes.

3.2 Typical metro station of the Grand Paris Express project

3.2.1 Geometry, boundary conditions and ground parameters

Table 1 and Fig.2 show the geometry and the boundary conditions of the model. Table 2 gives the geology and the thermo-hydraulic parameters used. The mesh is refined close to the diaphragm walls and it includes 411 450 nodes and 398 800 zones.

Table 1: Geometry and boundary conditions

Properties	Diaphragm wall	Base slab	Boundaries	
Length [m]	100	100	+ 115 from diaphragm wall downstream/+ 385 from diaphragm wall upstream	
Width [m]	30	30	+ 110 from diaphragm wall	
Depth [m]	58	30	+ 22 from diaphragm wall	
Thickness [m]	0.8	1	-	

	Boundary conditions	Symbol	Unity	Value
Thermal	Initial temperature	T_{ave}	[°C]	14
	Seasonal variation of temperature	$T_{surface}$	[°C]	2 (winter) – 26 (summer)
	Temperature of the substratum	$T_{substratum}$	[°C]	14
	Temperature of the edges	T_{edge}	[°C]	-
	Heat exchange convective coefficient	h_{conv}	[W/m ² .K]	1
	Inside air temperature	T_{air}	[°C]	20
	Damping depth	d	[m]	3
Hydraulic	Minimal water head	h_{min}	[m]	75
	Maximal water head	h_{max}	[m]	77

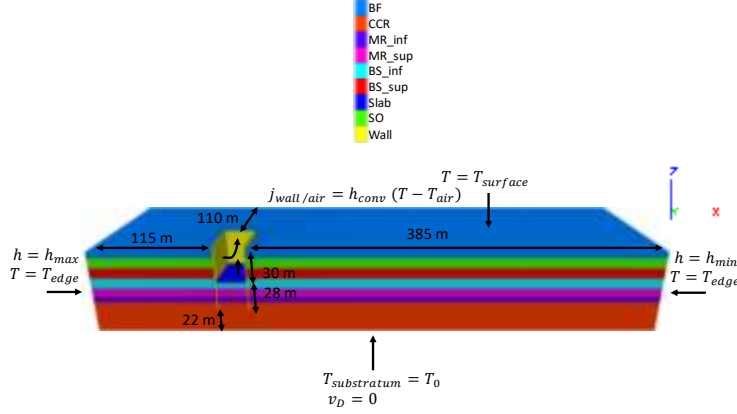


Fig. 2: cross-section of the metro station 3D model

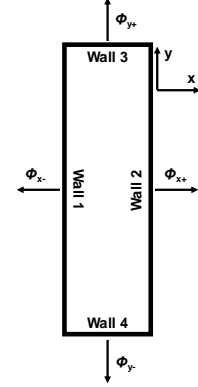


Fig. 3: position of the walls and heat fluxes

Table 2: geology and thermo-hydraulic parameters

Geology	BF	SO	BS _{sup}	BF _{inf}	MR _{sup}	MR _{inf}	CCR
Thickness [m]	6	10	10	11	5	15	> 10
Hydraulic conductivity [m/s]	1.10^{-5}	2.10^{-5}	1.10^{-5}	3.10^{-6}	1.10^{-3}	1.10^{-3}	2.10^{-4}
Thermal conductivity [W/m/K]	1.7	2.1	2.3	2.3	2.1	2.1	2.4
Volumetric heat capacity [MJ/m ³ /K]	2.2	2.2	2.3	2.3	2.2	2.2	2.2

3.2.2 Results

After the initialisation of the groundwater flow and the temperature field, a thermal solicitation is applied to the diaphragm walls at 20 cm from the interface ground/structure for ten years (see Fig. 4). Two signals are tested: a sinusoid perfectly balanced and a real solicitation with more heating than cooling on one year and with thermal rest during the night and the week-end.

Fig. 5 presents the mean daily heat exchange calculated on one year $\bar{P}_{tot,year}$ ($W_{day/year}$) for the overall metro station and the four diaphragm walls for the sinusoidal solicitation. For the first year, the values are positive showing a decrease of temperature in the control volume. The values tend to decrease year after year until it reached zero at the fifth year. It can be concluded that there is no thermal drift in this control volume and consequently, at the scale of the structure. Indeed, the heat injected in the ground is stored during the cooling period (the first six month of the sinusoid) before its use during winter. As a result, the ground reaches the steady state after few cycles. Moreover, the temperature of the system is in the

right range (+1/+35 °C) and the heat exchanges are mainly conductive due to the hydraulic context.

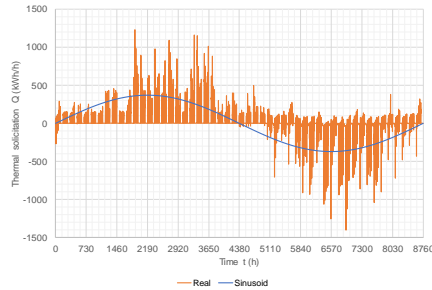


Fig. 4: thermal solicitations apply to the diaphragm walls

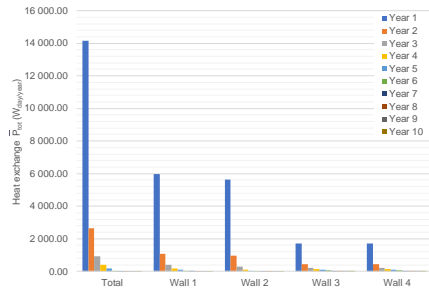


Fig. 5: heat exchange based on the divergence approach – sinusoidal solicitation

However, locally, in the zones where the groundwater flow velocity is the highest (on the corner), the advection is non-negligible, counting for 30% of the heat exchanges. In these zones, the heat cannot be stored and is dissipated by the groundwater flow leading to extreme temperature. Indeed, as there is no more reserve, the ground has to provide more heating or cooling.

Fig. 6 presents the mean daily heat exchange calculated on one year $\bar{P}_{tot,year}$ ($W_{day/year}$) for the overall metro station and the four diaphragm walls for the real solicitation. Year after year, the values increased leading to a progressive cooling of the control volume. The steady state is not reached after ten years. However, the cooling decreased slowly. Furthermore, the thermal drift is higher at the wall 1 (upstream) and 2 (downstream) where the groundwater flow is the lowest due to the dam effect of the structure. **Fig. 7** presents the ratio between the mean seasonal heat flux on one year $\bar{\Phi}_{year}$ ($W/m^2_{3month/year}$) and the maximum mean seasonal heat flux on one year $\bar{\Phi}_{max,year}$ ($W/m^2_{3month/year}$) for the wall 1. It highlights the decrease of the performance related to the thermal drift. After ten years, the decrease of the performance of the system reached 10 % for the autumn. These results are dependant of the thermal solicitation and of the wall.

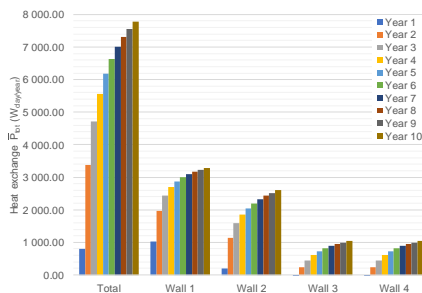


Fig. 6: heat exchange based on the divergence approach – real solicitation

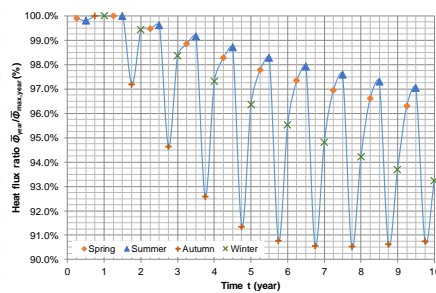


Fig. 7: decreasing of the thermal performance related to the thermal drift – wall 1

4. Conclusion

The methodology developed in this paper aims at the assessment of the heat exchange between a thermoactive geostructure and the ground considering the heat conductive flux and the advective flux due to the groundwater flow velocity. The results highlight the zones and the conditions where the thermal drift is likely. Thereby, in the case of a perfectly balanced energy demand, the system does not drift and the steady-state is reached after few years. In the case of an unbalanced thermal solicitation, the temperature around the structure increases or decreases along the years, leading to lower and lower performances of the system. In each case, the heat exchange is function of the depth and of the diaphragm wall.

5. References

- Adam D., & Markiewicz R. (2009). Energy from earth-coupled structures, foundations, tunnels and sewers. *Géotechnique*, 59(3): 229-236.
- Barla M., Di Donna A. & Perino A. (2016). Application of energy tunnels to an urban environment. *Geothermics*, 61: 104-113.
- Brandl H. (2006). Energy foundations and other thermo-active ground structures. *Géotechnique*, 56(2): 81-122.
- Campanella R.G. & Mitchell J.K. (1968) Influence of temperature variations on soil behavior. *Journal of soil mechanics and foundation division ASCE*, 94(3): 709-734.
- CFMS et SYNTEC. (2017). Recommandations pour la conception, le dimensionnement et la mise en oeuvre des géostructures thermiques. *Revue Française de Géotechnique*, 149, 120 p.
- Di Donna A., Rotta A.F., & Laloui L. (2016). Numerical study of the response of a group of energy piles under different combinations of thermo-mechanical loads. *Computers and Geotechnics*, 72: 126-142.
- FLAC3D Version 5.01 User's guide (2013), Minnesota, USA: ITASCA Consulting Group, Inc.
- Fromentin A., & Pahud D. (1997). Recommandations pour la réalisation d'installations avec pieux échangeurs. Rapport final. Rapport d'étude n°120.104. Office fédéral de l'énergie, Lausanne, Suisse. 79 p.
- Laloui L., & Cekerevac C. (2008). Numerical simulation of the non-isothermal mechanical behavior of soils. *Computers and Geotechnics*, 35: 729-745.
- Pahud D., Fromentin A., & Hubbuch M. (1999). Heat exchanger pile system of the dock midfield at the Zürich Airport. Detailed simulation and optimization of the installation. Rapport final. Rapport d'étude n°120.110. Office fédéral de l'énergie, Lausanne, Suisse. 49 p.
- Signorelli S., Bassetti S., Pahud D. & Kohl T. (2007). Numerical evaluation of thermal response tests. *Geothermics*, 36: 141-166.
- Xia C., Sun M., Zhang G., et al. (2012). Experimental study on geothermal heat exchangers buried in diaphragm walls. *Energy and Buildings*, 52: 50-55.
- Zarella A., Emmi G., Zecchin R. & De Carli M. (2017). An appropriate use of thermal response test for the design of energy foundation piles with U-tube circuits. *Energy and buildings*, 134: 259-270.